Rouse and Reptation Dynamics at Finite Temperatures: A Monte Carlo Simulation

J. Wittmer,† W. Paul,* and K. Binder

Institut für Physik, Universität Mainz, D-6500 Mainz, Germany

Received June 15, 1992; Revised Manuscript Received September 8, 1992

ABSTRACT: The temperature dependence of the dynamics of polymer chains in the melt is studied in a Monte Carlo simulation of the bond fluctuation model. Temperature enters via a bond angle potential determining the stiffness of the chains. The model is simulated at a melt volume fraction of $\Phi = 0.5$ and for chains of lengths $N = 20, 50, 100$, and 200. For the short chains we are determining the temperature range over which a random coil description of these semiflexible chains is possible, i.e. the temperature region for which the chains show the behavior of random coils in the melt. We then examine to what extent the Rouse model is able to describe the dynamics of these chains. We will look especially at the Rouse scaling for the dynamic structure factor. For the longest chains it has been shown that our model in the athermal limit can be described by the reptation picture of DeGennes and Doi and Edwards and the density dependence of the tube diameter has been established. Here we now measure the temperature dependence of this dynamic length scale by analyzing the dynamic structure factor. It is shown to decrease slightly with decreasing temperature in accord with recent findings of neutron spin echo experiments.

1. Introduction

The proper description of the dynamics of polymer chains in the melt is still an unsolved problem. For their static properties one knows that the global conformational properties of the chains can be described by Gaussian statistics as soon as the excluded volume screening length, that is the distance in space over which the mutual nonbonded interaction between monomers is screened, is small enough, i.e. of the order of the persistence length. These seemingly random walk chains then should be describable by the Rouse model,[1] a chain of noninteracting beads coupled by harmonic springs and in contact with a heat bath. As long as the chains are short enough, viscoelastic properties[2] like the chain length dependence of the viscosity support this description. Furthermore recent neutron spin echo experiments[3] on PDMS showed that the decay of the dynamic structure factor follows the scaling[4,5] derivable from the eigenmodes of the Rouse chain. For longer chains the mutual hindrance of the chains and the topological properties of a thread become noticeable. In this regime the reptation concept[5-7] is the most successful in describing the viscoelastic and dynamic behavior. In this single chain description the motion of a chain at intermediate times is postulated to be confined to a tube built up by the topological constraints through the neighboring chains and thus to follow a one-dimensional path in space. As the reptation concept fails to predict the $M^{3.4}$ dependence experimentally found for the viscosity and instead comes up with a M^3 behavior, the underlying microscopic picture has been heavily challenged.[8-12] However, a series of recent computer simulations and experiments found ample evidence for the validity of the reptation concept in the following respect. All the evidence amounts to the existence of a chain length independent purely dynamic length scale in polymer melts which we will call tube diameter. Kremer and Grest[13] in a molecular dynamics (MD) simulation showed the existence of the crossover to a geometrically constrained motion at the entanglement time τ_e and measured the corresponding tube diameter. Paul et al.[14,15] in a Monte Carlo simulation of the bond fluctuation model determined the density dependence of the tube diameter and showed that it is proportional to the screening length. Furthermore, they established the second dynamic crossover predicted by the reptation theory. Neutron scattering experiments[16,17] had been able to show a deviation from Rouse behavior in the decay of the dynamic structure factor, and recently, Richter et al.[18] have been able to measure the temperature dependence of the tube diameter in a melt of poly(ethylene–propylene) chains. Reptation theory successfully accounted for this dynamical length scale and the measured ratio between the two crossover times τ_R/τ_e observed in ref 14. Hess[19] in a series of papers using a projection operator formalism starting from the microscopic dynamics has rederived the reptation scenario by assuming invariance against curvilinear displacements of the forces at chain contact points and employing suitable decoupling approximations. It has been argued (for instance refs 15 and 20) that the discrepancies in predicting the viscosity are due to the single chain level of description of reptation theory. We will take up this point of view in this paper and pursue it by analyzing the shortcomings and successes of the Rouse description of short chain dynamics which suffers from the same problems but is more accessible. This analysis will furnish a sound basis for the interpretation of the data for the long chains where we will determine the temperature dependence of the tube diameter in the same way as it was done in the neutron spin echo experiments.

The organization of this paper is as follows. In section 2 we will describe our model and give technical details on the algorithm and simulation technique. Section 3 presents a discussion of the static properties of the chains where we determine down to which temperature they can be described as Gaussian coils with a temperature-dependent statistical segment length. For this temperature range the dynamic behavior of short chains is analyzed in section 4 and the validity of the Rouse scaling for the dynamic structure factor is shown. In contrast to experiment, this scaling can be done without free parameters because all quantities are independently measurable in the computer simulation. Furthermore, we will give a detailed check of the Rouse predictions for the self-diffusion of the chains. Section 5 finally contains our data for the well-entangled chains of length $N = 200$ and a determination of the tube diameter from the dynamic structure factor.

† Present address: Institue Charles Sadron, 67083 Strasbourg, France.

0024-9297/92/2225-7211$03.00/0

2. Model and Algorithm

We have used the three-dimensional version of the bond fluctuation model[21] for our simulation. A detailed discussion of the model has been given in refs 22 and 23, so we will only give a brief description and focus on the inclusion of temperature. In this model each repeat unit or monomer occupies the eight corners of the unit cube on the simple cubic lattice. The bonds between adjacent monomers can vary in length and direction subject only to excluded volume constraints and entanglement restrictions. This leaves one with 5 possible bond lengths (2, $\sqrt{5}, \sqrt{6}, 3, \sqrt{10}$; all lengths being measured in units of the lattice spacing) and 87 possible angles between consecutive bonds. The elementary moves of the monomers are random hoppings to nearest neighbor sites. It has been shown[23] that excluded volume then forbids any intersection of bonds throughout the random motion of the polymers.

In an experimental system the temperature influences the conformational properties of a single chain as well as the overall density and density fluctuations in the melt. Both have an effect on the chain dynamics and consequently on the question of entanglement effects. In the simulation we will deal with an N, V, T ensemble, thus neglecting the effect of a density variation. Thus our simulation will separate out the effect of the chain stiffness on the single chain dynamics both in the Rouse and the reptation regime.

The effect on the chain conformation of cooling the melt is to prefer the absolute minimum of the torsion angle potential; i.e. the chain stiffens. As one can visualize one repeat unit of the lattice model to represent a group of atoms in a real chain, we can model this stiffening by choosing a potential for the bond angles that prefers straight conformations.[24,25] A particularly simple choice is

$$E(\alpha) = \epsilon \cos \alpha \tag{1}$$

where α is the complementary angle to the one enclosed by consecutive bonds $\vec{l}, \vec{l}'$. In addition to excluded volume restrictions and restrictions on the set of allowed bonds, each move is now only accepted according to the Metropolis rate

$$W_{\mathrm{Met}} = \frac{1}{\tau} \min\left(1, \exp\left(-\frac{\Delta E}{k_{\mathrm{B}} T}\right)\right) \tag{2}$$

Note that each of the described elementary moves alters three adjacent bond angles. From now on temperature will be measured in units of the strength ϵ of the bond angle potential and Boltzmann's constant is $k_{\mathrm{B}} = 1$.

In ref 14 it was shown that for the bond fluctuation model a polymer volume fraction of $\Phi = 0.5$ represents a polymer melt with an excluded volume screening length of about two bond lengths. Therefore we chose $\Phi = 0.5$ to study the influence of temperature on the dynamics of chains in the melt. We started the simulations with equilibrated samples of athermal systems ($1/T = 0$) and then employed a stepwise cooling procedure equilibrating the system at each respective temperature. This paper will concentrate on the temperature range $1/T \in [0, 1]$, but for the shortest chains of $N = 20$ we cooled the system down to $1/T = 10$. For the lower temperatures we get a crossover to semirigid chains of only a few statistical segment lengths and an accompanying nematic ordering phenomenon.[25] In the temperature range $1/T \in [0, 1]$ we studied the static and dynamic properties of the chains of lengths $N = 20$, 50, 100, and 200 on a periodic lattice of linear size $L = 40$. For $N = 20$, 50, and 100 all dynamical measurements were done after equilibrating the samples so that we study equilibrium dynamics. For $N = 200$ we were only able to equilibrate the chains locally so that they showed the correct temperature-dependent persistence length. Lack of equilibration on scales of the order of the chain end-to-end distance does not matter too much, however, since we are mostly interested in the short time dynamics of monomer displacements. These short-scale phenomena are hardly affected by the degree of equilibration on much longer scales, as test runs showed.

This algorithm was implemented on the Multitransputer Facility of the Condensed Matter Theory group in Mainz.[14] Each T800 transputer got his own system to work on, and we employed the parallelization to improve the statistics of the data running typically 17 systems in parallel. Each of the 17 systems then contained 200 chains for $N = 20$, 80 chains for $N = 50$, 40 chains for $N = 100$, and 20 chains for $N = 200$.

3. Static Properties in the Random Coil Regime

The bond angle potential we employ tends to straighten out the chains when we lower the temperature, preferring a stretched configuration for each pair of successive bonds. Even at infinite temperature the characteristic ratio

$$c_N \equiv \langle R^2 \rangle / (N-1) \langle l^2 \rangle \tag{3}$$

is bigger than one in the bond fluctuation model. Therefore the number of statistical segments per chain N' is smaller than the number of bonds $N - 1$.

$$N' = (N-1)/c_N \tag{4}$$

One will be able to find the random coil behavior as long as the number of statistical segments is "large enough", say larger than 10. A simple analytical description of the chain stretching is possible by assuming the bond angles along the chain to be independent. As the excluded volume screening length at the simulated polymer volume fraction is about two bond lengths, an approximation in the form of independent trimers seems reasonable. In this case one can follow the Flory[26] calculation to derive the characteristic ratio

$$c_N = \frac{1 - \langle \cos \alpha \rangle}{1 + \langle \cos \alpha \rangle} + \frac{2 \langle \cos \alpha \rangle}{N-1} \frac{1 - (-\langle \cos \alpha \rangle)^{N-1}}{(1 + \langle \cos \alpha \rangle)^2} \tag{5}$$

Here $\langle \cos \alpha \rangle$ is the thermal average for a bond angle. In the same approximation this is given as

$$\langle \cos \alpha \rangle = \frac{1}{Z} \sum_{i=1}^{87} g_i \cos \alpha_i \exp\left(-\frac{1}{T} \cos \alpha_i\right) \tag{6}$$

where the summation is over the 87 different bond angles in the bond fluctuation model, g_i is the degeneracy of the angle α_i, i.e. the number of pairs of bonds $(\vec{l}, \vec{l}')$ giving the same bond angle, and Z is the partition sum for a single angle

$$Z = \sum_{i=1}^{87} g_i \exp\left(-\frac{1}{T} \cos \alpha_i\right) \tag{7}$$

Figure 1 is a plot of the measured mean cosine for $N = 20$ compared to the prediction of eq 6. The agreement over the whole temperature range is excellent even though at the lowest temperatures the chains are already very much stretched out and consist of only 3 statistical segment lengths, as can be seen in Table I. Here we compare the characteristic ratio predicted by eq 5 to the one measured in the simulation and again the agreement is excellent. Table I also includes the measured mean value for the bond angle to help visualize the local stretching. From

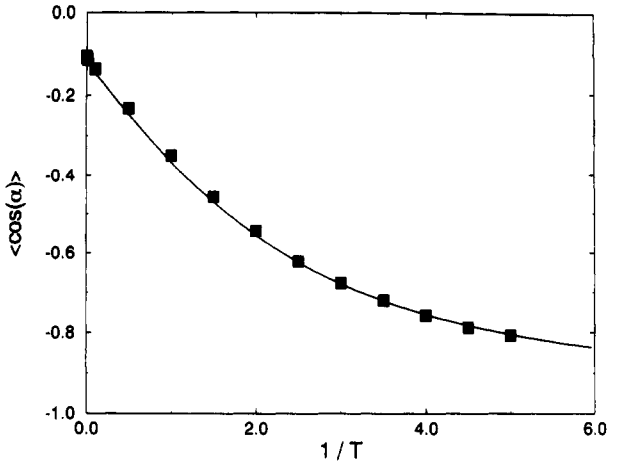

Figure 1. Mean value of cos α plotted versus inverse temperature. Squares denote simulation measurements; the full curve is the prediction from eq 6.

Table I
Average Angle [α] (deg) Observed in the Simulations and the Characteristic Ratio According to eq 5 (c_N^{theor}) as Well as the One Measured in the Simulations[a]

$1/T$	[α]	C_N^{theor}	$c_N \doteq \langle R^2\rangle/(N-1)\langle l^2\rangle$
0.0	97.83 ± 0.15	1.26	1.32 ± 0.02
0.001	98.07 ± 0.14	1.26	1.303 ± 0.002
0.01	98.29 ± 0.14	1.26	1.366 ± 0.007
0.1	99.73 ± 0.15	1.32	1.39 ± 0.02
0.5	106.19 ± 0.05	1.61	1.60 ± 0.02
1.0	114.08 ± 0.05	2.06	1.98 ± 0.01
1.5	121.42 ± 0.02	2.59	2.49 ± 0.01
2.0	127.71 ± 0.01	3.20	3.04 ± 0.02
2.5	133.39 ± 0.15	3.85	3.756 ± 0.002
3.0	137.51 ± 0.02	4.53	4.377 ± 0.002
3.5	141.00 ± 0.02	5.20	5.09 ± 0.02
4.0	144.11 ± 0.01	5.85	5.88 ± 0.04
4.5	146.75 ± 0.23	6.47	6.21 ± 0.17
5.0	148.56 ± 0.25	7.05	6.99 ± 0.16

[a] Temperatures are quoted in units of ϵ.

these data one can conclude that we will be able to treat even our smallest chains of $N = 20$ as random coils as long as we restrict the temperature range to $1/T \in [0, 1]$. This is also supported by the single chain structure factor which is plotted for $1/T = 1.0$ in Figure 2. Included is the random coil prediction for the self-similar regime.

In the following section we will look at the dynamics of the short chains in this temperature range.

4. Dynamics of Short Chains in the Melt

In this section we will look at the melt dynamics of the chains of length $N = 20$, 50, and 100 and focus on the temperature range $1/T \in [0, 1]$. We will look at the diffusion of the chains as a whole and of single monomers in the chains and examine the behavior of the dynamic structure factor. The dynamics of short chains in the absence of hydrodynamic interactions is usually described with the Rouse model. In this model one can derive a lot of interdependent results on the diffusive behavior of the chains and it predicts a special scaling form for the dynamic structure factor at short times. Let us first review the predictions we want to analyze in the simulation. Rouse dynamics in the Einstein–Smoluchowski description of a chain of point particles connected by harmonic springs. If $\vec{r}_n$ is the position of the nth bead, it follows the equation of motion[5]

$$\zeta \mathrm{d}\vec{r}_n = \frac{3k_BT}{\sigma^2}(\vec{r}_{n+1} - 2\vec{r}_n + \vec{r}_{n-1})\mathrm{d}t + \mathrm{d}\vec{w}_n(t) \qquad (8)$$

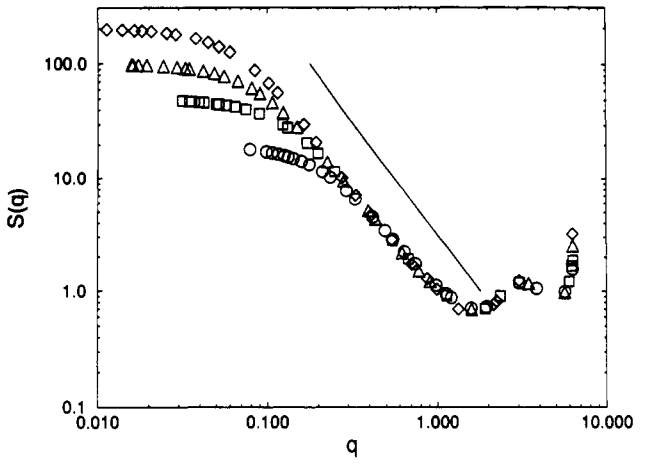

Figure 2. Single chain structure factor at $1/T = 1$ for chains of length $N = 20$ (circles), 50 (squares), 100 (triangles), and 200 (diamonds). The straight line indicates the q^{-2} behavior for a Gaussian chain.

where ζ is the monomeric friction coefficient, σ is the statistical segment length of the chain, and $\mathrm{d}\vec{w}_n$ are Wiener processes in three-dimensional space obeying

$$\langle \mathrm{d}\vec{w}_n(t)\rangle = 0$$

$$\langle \mathrm{d}w_{n\alpha}(t)\mathrm{d}w_{m\beta}(t')\rangle = \begin{cases} 0 & t \neq t' \\ 2\zeta k_BT\delta_{nm}\delta_{\alpha\beta} & t = t' \end{cases} \qquad (9)$$

where α and β are Cartesian coordinates. As there is no net force acting on a chain, the center of mass of a chain performs a free diffusion at all times.

$$g_3(t) \doteq \langle(\vec{r}_{cm}(t) - \vec{r}_{cm}(0))^2\rangle = 6D_{N'}t \qquad (10)$$

with the chain center of mass diffusion coefficient

$$D_{N'} = k_BT/N'\zeta \qquad (11)$$

Equation 8 is solvable by an eigenmode analysis where the longest relaxation time is the Rouse time:[1,5]

$$\tau_R = \frac{1}{3\pi^2}\frac{\zeta}{k_BT}\sigma^2N'^2 \qquad (12)$$

Note that

$$g_3(\tau_R) = \frac{2}{\pi^2}N'\sigma^2 = \frac{2}{\pi^2}\langle R^2\rangle \qquad (13)$$

where $\langle R^2\rangle$ is the mean squared end-to-end distance.

From the eigenmode analysis one furthermore gets an equation for the mean square displacement of the nth statistical segment relative to the position of the mth statistical segment at $t = 0$.

$$\Phi_{nm}(t) \doteq \langle(\vec{r}_n(t) - \vec{r}_m(0))^2\rangle$$

$$= 6D_{N'}t + |n-m|\sigma^2 +$$

$$\frac{4N'\sigma^2}{\pi^2}\sum_{p=1}^{\infty}\frac{1}{p^2}\cos\left(\frac{p\pi m}{N'}\right)\cos\left(\frac{p\pi n}{N'}\right)\left(1 - \exp\left(-\frac{p^2t}{\tau_R}\right)\right) \qquad (14)$$

For $n = m$ and $t \ll \tau_R$ this reduces to

$$\Phi_{nn}(t) = \sigma^2\sqrt{Wt} \qquad (15)$$

where W is the Rouse rate setting the microscopic time scale for the diffusive processes.

$$W = \frac{12}{\pi}\frac{k_BT}{\zeta\sigma^2} \qquad (16)$$

In the simulation the statistical segment length σ^2 is

measured from the static quantities. The self-diffusion coefficient of the chains $D_{N'}$ is measured from the mean square displacement

$$D_{N'} = \lim_{t\to\infty} g_3(t)/6t \tag{17}$$

The Rouse time τ_R is either accessible by using eq 13 or by studying the correlation function of the end-to-end vector of the chains

$$\Phi_{EE}(t) \doteq \langle(\vec{r}_{N'}(t) - \vec{r}_1(t))\cdot(\vec{r}_{N'}(0) - \vec{r}_1(0))\rangle$$
$$= N'\sigma^2 \sum_{p=1,3,\ldots} \frac{8}{p^2\pi^2} \exp\left(-\frac{p^2 t}{\tau_R}\right) \tag{18}$$

Thus, neglecting the higher eigenmodes

$$\int_0^\infty \frac{\Phi_{EE}(t)}{\Phi_{EE}(0)}\,dt \approx \tau_R \tag{19}$$

Note that eqs 11, 12 and 16 imply the following relation

$$\frac{k_B T}{\zeta} = N' D_{N'} = \frac{\sigma^2 N'^2}{3\pi^2 \tau_R} = \frac{\pi}{12}\sigma^2 W \tag{20}$$

For ideal Rouse chains one can explicitly calculate the dynamic structure factor

$$S(q,t) = \frac{12}{q^2\sigma^2}\int_0^\infty \exp(-u - \sqrt{\Gamma_q t}\,h(u(\Gamma_q t)^{-1/2}))\,du \tag{21}$$

where the function h is given as

$$h(u) = \frac{2}{\pi}\int_0^\infty \frac{\cos(xu)}{x^2}(1 - \exp(-x^2))\,dx \tag{22}$$

and the rate Γ_q is defined as

$$\Gamma_q = \frac{\pi}{144} q^4 \sigma^4 W \tag{23}$$

In the time regime where $1 \ll \Gamma_q t \ll \Gamma_q \tau_R$ this can be further simplified to give

$$\frac{S(q,t)}{S(q,0)} = \exp\left(-\frac{2}{\sqrt{\pi}}(\Gamma_q t)^{1/2}\right) \tag{24}$$

The above equations imply that at short times $S(q,t)$ plotted versus $q^4\sigma^4 W t$ should yield a universal curve independent of the q value or the temperature under study. This scaling in the short time decay of the dynamic structure factor has been nicely verified in a neutron spin echo experiment on a PDMS melt[3] where the quantity $\sigma^4 W$ served as a fitting parameter. In the simulation we will calculate the intermediate scattering function by assigning one scattering center to each repeat unit of the lattice chains.

Note that we deliberately used N' and σ to denote the Rouse chain. What we have in mind is the concept of an equivalent Rouse chain composed of $N' = (N-1)/c_N$ statistical segments σ having the same dynamic behavior as our simulated lattice chains on length scales larger than $\sigma = c_N\langle l^2\rangle^{1/2}$ and time scales larger than $1/W$. The analysis of the measurements on the simulated lattice chains can only be done after translation into the properties of this equivalent Rouse chain. Let us now first study the diffusive behavior of the chains.

For the simulated lattice chains we define the following mean square displacements.[14]

Mean square displacement of the inner monomers

$$g_1(t) \doteq \frac{1}{5}\sum_{i=N/2-2}^{N/2+2} \langle(\vec{r}_i(t) - \vec{r}_i(0))^2\rangle \tag{25}$$

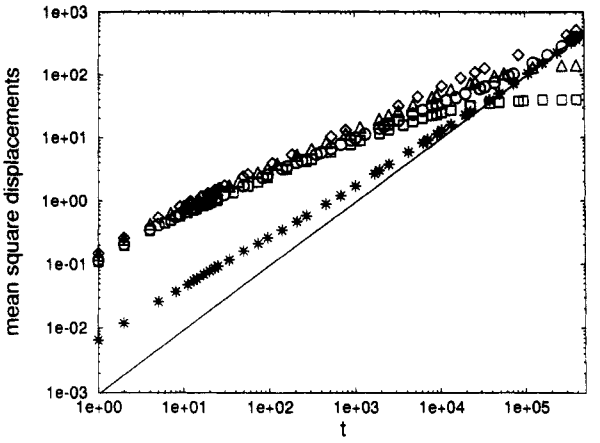

Figure 3. Various mean square displacements measured for the Rouse-like chains of $N = 20$ at $T = 1$ plotted versus time measured in MCS: g_1 (circles); g_2 (squares); g_3 (stars); g_4 (triangles); g_5 (diamonds). Also included is the asymptote $6D_{N'}t$ of $g_3(t)$. For the definition of g_1–g_5 see the text.

The same in the center of mass coordinate frame

$$g_2(t) = \frac{1}{5}\sum_{i=N/2-2}^{N/2+2} \langle[\vec{r}_i(t) - \vec{r}_{cm}(t) - \vec{r}_i(0) + \vec{r}_{cm}(0)]^2\rangle \tag{26}$$

Mean square displacement of the center of mass (eq 10)

$$g_3(t) = \langle(\vec{r}_{cm}(t) - \vec{r}_{cm}(0))^2\rangle \tag{27}$$

Mean square displacement of the end monomers

$$g_4(t) \doteq \frac{1}{6}\sum_{i=1-3,N-2,N-1,N} \langle(\vec{r}_i(t) - \vec{r}_i(0))^2\rangle \tag{28}$$

The same in the center of mass coordinate frame

$$g_5(t) \doteq \frac{1}{6}\sum_{i=1-3,N-2,N-1,N} \langle[\vec{r}_i(t) - \vec{r}_{cm}(t) - \vec{r}_i(0) + \vec{r}_{cm}(0)]^2\rangle \tag{29}$$

Due to the averaging over several monomers g_1, g_2, g_4, and g_5 can be interpreted as the mean square displacements of central respectively end segments of the equivalent Rouse chains (it also helps to improve the statistics). Figure 3 is a plot of g_1–g_5 versus time (measured in Monte Carlo steps). The shape of the curves is the same as the exact result for the Rouse model. In ref 15 characteristic times for the Rouse model were defined by

$$g_1(\tau_1) = \langle R_G^2\rangle \tag{30}$$

$$g_2(\tau_2) = {}^2/_3\langle R_G^2\rangle \tag{31}$$

$$g_3(\tau_3) = g_2(\tau_3) \tag{32}$$

$$g_5(\tau_4) = \langle R_G^2\rangle \tag{33}$$

It was found that in a melt the ratios τ_i/τ_j differ from the exact results for the Rouse model. Table II gives the Rouse prediction for some of these ratios and the measured ratios in the temperature range $1/T \in [0,1]$. In the range where the Rouse model is expected to be a valid description of the chain dynamics the ratios do not depend on temperature, that is the characteristic times all have the same temperature dependence. Note that in the temperature interval shown N' already varies significantly since c_N increases by about 50% from the athermal case to $T = 1$. When the temperature is reduced even further, the chain of length $N = 20$ no longer contains enough statistical

Table II
Acceptance Rate A and the Characteristic Time τ_1 (MCS) as Well as Its Ratio with the Other Characteristic Times Defined for the Rouse Model (See Text)[a]

$1/T$	A	τ_1	τ_2/τ_1	τ_3/τ_1	τ_4/τ_1
Rouse			0.740	3.726	0.289
0.0	0.1607	6800 ● 300	0.98	2.4	0.59
0.001	0.1601	6700 ● 300	0.97	2.5	0.61
0.01	0.1600	6600 ± 300	1.03	2.5	0.62
0.1	0.1583	7000 ± 200	0.98	2.5	0.62
0.5	0.1501	9900 ± 300	1.01	2.3	0.57
1.0	0.1395	15200 ± 200	1.07	2.2	0.54

[a] The chain length is $N = 20$. Results are given for the ideal model and the simulated melt systems at the respective temperatures.

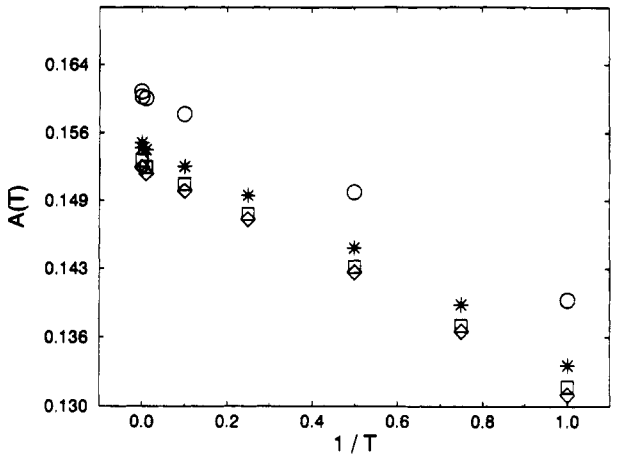

Figure 4. Acceptance rate $A(T)$ in the Monte Carlo procedure as a function of inverse temperature for $N = 20$ (circles), $N = 50$ (stars), $N = 100$ (squares), and $N = 200$ (diamonds).

segments to behave like a Rouse chain and the above defined relaxation times even change their ordering.[25]

The temperature dependence can be understood by looking at the acceptance rate of the Monte Carlo procedure (Figure 4). It shows a clear Arrhenius behavior with an activation energy of $\Delta E_A = 0.14$ (in units of ϵ) reflecting the effect of the bond angle potential on the Monte Carlo moves. The chain length dependence of the acceptance rate is an effect of the end monomers that are more mobile than the inner monomers (compare $g_1(t)$ and $g_4(t)$). The same holds for the temperature dependence of the chain self-diffusion coefficient (Figure 5, $\Delta E_D = 0.4$) so we are sure not to be influenced by effects of a dynamic freezing due to a glass transition in the model.[27-30]

The shortcomings of the single chain description can most prominently be seen in the short time behavior of the mean square displacement of the center of mass of the chains. This displays no free diffusion but is proportional to t^x with $x < 1$. Reference 14 discussed the density dependence of this effect. In Figure 6 we show the short time mean square displacement of the chains of length $N = 20$ at various temperatures in the considered interval. There is an indication of a slight decrease of the effective exponent with decreasing temperature, but within the error bars all curves are compatible with the exponent $x = 0.85$ found for $1/T = 0$. The same holds true for the chains of length $N = 50$ and $N = 100$.

Therefore one concludes that there is a net force acting on the center of mass of the chains and it is generated by the chain movement itself. In the Monte Carlo simulation we see a strong enhancement of the back-jump probability for the monomers, that is, each successful monomer move is more likely to be the reverse one to the one made before than any one of the other five possibilities tried with the same probability. This is a strong effect, as can be seen

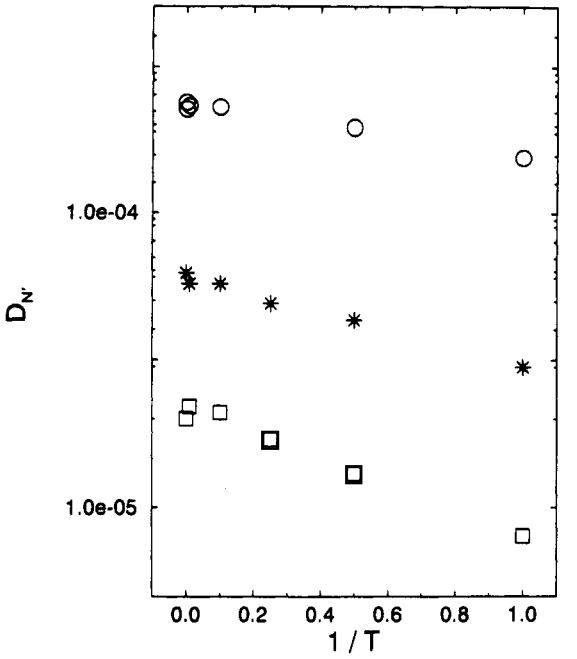

Figure 5. Center of mass diffusion coefficient of the chains as a function of inverse temperature for $N = 20$ (circles), $N = 50$ (stars), and $N = 100$ (squares).

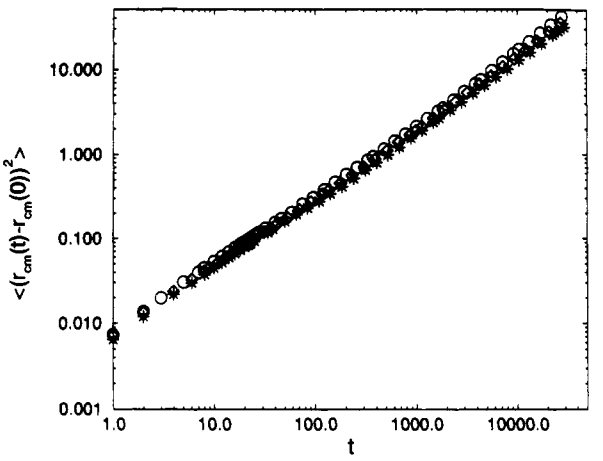

Figure 6. Small time mean square displacements of the center of mass of the chains for $1/T = 0.0$ (circles), 0.5 (diamonds), and 1.0 (stars) and $N = 20$.

from a comparison between the Rouse rate, W, and the acceptance rate, A. The latter is $100(1/T = 0)$ to $1000(1/T = 1)$ times larger than the former, showing that there is an interchain (excluded volume interactions) as well as an intrachain (chain stiffness) part to this effect. For this reason the center of mass diffusion, $g_3(t)/t$, starts off at a value of A/N and reaches a free diffusion plateau proportional to W for $t \to \infty$.[15] For the static chain conformation we know that all the excluded volume forces effectively cancel and the chain statistics look as if there are no interactions at all. Therefore let us ask the question whether this is also true for the changes of the chain conformation in its center of mass coordinate frame, that is whether the Rouse description is valid here. There have been detailed studies of the eigenmodes of chains in a computer simulation for instance,[9,13,21] finding the Rouse modes on length scales larger than σ and on time scales larger than $1/W$. We will address this question first by looking at the predictions of eq 20. We therefore will calculate the Rouse rate W in several ways. Fitting eq 15 to $g_1(t)$ at short times gives W^{g_1}; measuring D_N according to eq 17 defines W^{D_N}, eq 19 yields W^{τ_R}, and eq 13 yields W^{g_3}. The resulting values are collected in Table III. Also

Table III
Various Ways To Extract the Rouse Rate W (cf. Text) from the Monte Carlo Simulation[a]

$1/T$	W^{g_1}	$W^{D_{N'}}$	W^{τ_R}	W^{g_3}	W^q
0.0	1.03×10^{-3}	8.4×10^{-4}	8.8×10^{-4}	8.8×10^{-4}	8.3×10^{-4}
0.001	9.5×10^{-4}	7.7×10^{-4}	8.3×10^{-4}	8.6×10^{-4}	6.5×10^{-4}
0.01	9.1×10^{-4}	7.4×10^{-4}	7.5×10^{-4}	8.2×10^{-4}	6.6×10^{-4}
0.1	8.0×10^{-4}	6.6×10^{-4}	7.0×10^{-4}	7.4×10^{-4}	5.1×10^{-4}
0.25	5.9×10^{-4}	4.6×10^{-4}	5.9×10^{-4}	5.6×10^{-4}	3.8×10^{-4}
0.5	3.6×10^{-4}	2.9×10^{-4}	3.5×10^{-4}	3.5×10^{-4}	1.7×10^{-4}
0.75	1.9×10^{-4}	1.7×10^{-4}	2.5×10^{-4}	1.9×10^{-4}	1.1×10^{-4}
1.0	1.2×10^{-4}	9.9×10^{-5}	1.4×10^{-4}	1.2×10^{-4}	6.3×10^{-5}

[a] Within the obtainable accuracy the first four rates coincide whereas the rate obtained from the structure factor shows a systematic deviation.

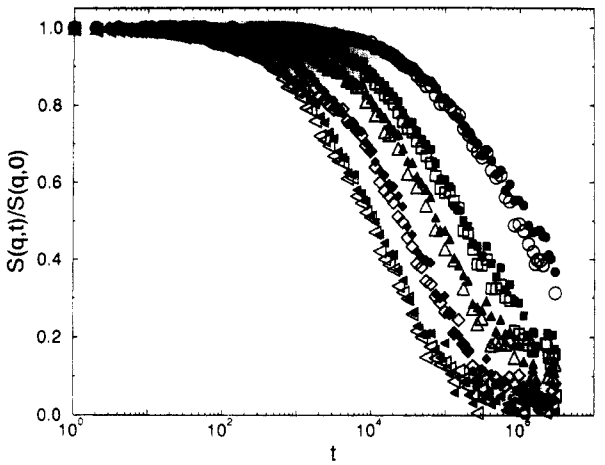

Figure 7. Dynamic structure factor for $N = 100$, $1/T = 1.0$, and $q_1 = 0.19$ (circles), $q_2 = 0.27$ (squares), $q_3 = 0.32$ (triangles pointing up), $q_4 = 0.4$ (diamonds), $q_5 = 0.49$ (triangles pointing left). Open symbols refer to scattering off the whole chain; closed symbols, to scattering off the $N/2$ monomers in the center of the chain.

included is a mean value for the Rouse rate W^q averaged over different W^{q_i} obtained by fitting the Rouse prediction (24) for the dynamic structure factor to the structure factor decay at the respective q value measured in the simulation. For this fitting procedure we used the simplified version eq 24 because of numeric instabilities with the more exact eq 21. In order to assert its range of validity one has to give a meaning to $\Gamma_q t \gg 1$. We used the condition $\Gamma_q t \geq 1$ and calculated Γ_q using the W^{g_1} measured from the monomer diffusion. There is, however, a strong dependence on the lower cutoff time whereas for a fixed cutoff the W^{q_i} values do not scatter very much so that we included only the mean value. Their temperature dependence differs, however, definitely from that of the W obtained out of the diffusion measurements. There seems to be roughly a factor of c_N between the two ways of measuring the Rouse rate. A factor between the rates W determined from the diffusion and the W^q has already been noted in experiments[17] and simulations.[13] The temperature dependence found here may be attributable to the fact that only every c_Nth scattering center along the chain moves statistically independently, but this point needs further study. The values for the Rouse rate obtained from the diffusion measurement compare very nicely and fulfill the consistency considerations in eq 20.

With the information on the statistical segment length and on the Rouse rate we can now proceed to analyze the dynamic structure factor. Figure 7 shows the raw data for the dynamic structure factor for $N = 100$ and $1/T = 1$ and several q values. It displays the scattering function of the whole chain (open symbols) as well as that of the inner half of the chain (closed symbols). Both scattering

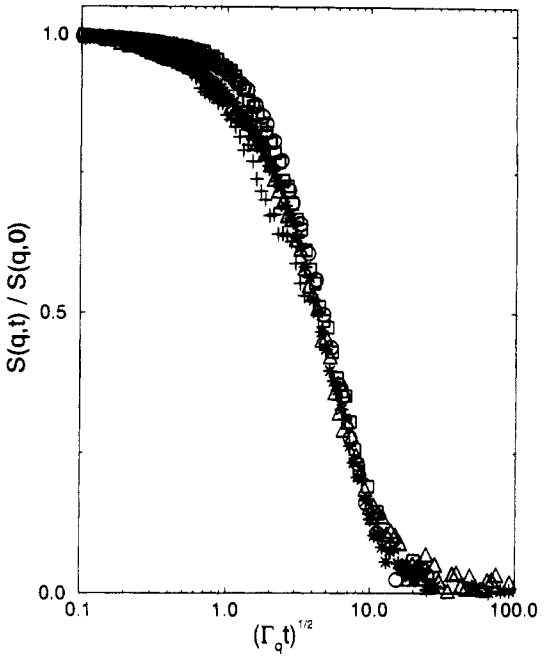

Figure 8. Rouse scaling of the dynamic structure factor for $N = 20$, $1/T = 0.0$, $q = 0.47$ (circles); $N = 20$, $1/T = 1.0$, $q = 0.8$ (stars); $N = 50$, $1/T = 0.0$, $q = 0.29$ (squares); $N = 50$, $1/T = 1.0$, $q = 0.7$ (triangles); $N = 100$, $1/T = 0.0$, $q = 0.47$ (diamonds); $N = 100$, $1/T = 1.0$, $q = 0.19$ (plus signs).

functions are identical for the length scales considered, showing no measurable influence of a faster decay of the correlations at the free chain ends. The test of the predicted Rouse scaling of the dynamic structure factor can now either be done by using the W^q as it was done in the experiment on PDMS[3] or with the independently measured Rouse rate from the diffusion data. Figure 8 shows the Rouse scaling for all our short chains $N = 20$, 50, and 100, the temperatures $1/T = 0$ and 1, and various q values. Only times smaller than $\tau_R(N,T)$ were included. We used the values of W^{g_3} to scale the abscissa. The predicted scaling is reproduced here without free parameters and nicely confirms the Rouse theory.

As a conclusion for the Rouse dynamics one can say that the conformational changes of the Gaussian chains in the melt are well described by the Rouse picture in spite of the fact that the interchain interaction leads to a net force on the center of mass of the chains at short times.

5. Melt Dynamics of Long Chains

Let us now finally examine the melt dynamics of the long chains of $N = 200$. These have been shown to be entangled in the athermal case.[14,15] Due to the slow reptative dynamics of these chains we were not able to equilibrate them by propagating each chain into the free diffusion limit. We therefore judged the equilibration by monitoring the characteristic ratio of the chains, the precise value of which we knew from the shorter chains and the analytical approximation. At each temperature the systems were equilibrated until this value was correct and consecutively the dynamics of the chains was studied.

In this section we will study the decay of the dynamic structure factor of the chains as has been done in the experiments on poly(ethylene–propylene).[18,33] Due to the occurrence of an additional dynamic length scale in the melts of entangled chains, the Rouse scaling which has the statistical segment length as the only relevant length scale is no longer valid. This is clearly displayed in Figure 9 which gives the rouse scaling plot for the chains of length

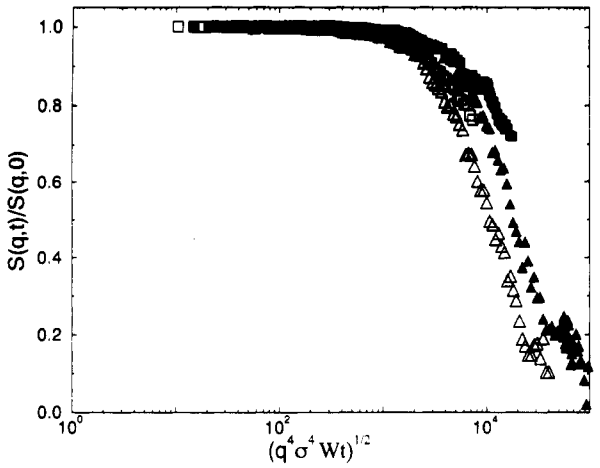

Figure 9. Failure of the Rouse scaling plot of the dynamic structure factor for $N = 200$. Data for $q = 0.15$ (squares) and $q = 0.35$ (triangles). Open symbols refer to $1/T = 0$; closed symbols, to $1/T = 1$.

$N = 200$. In the framework of the reptation picture De Gennes[4] has calculated the dynamic structure factor of a single chain. It reaches a plateau for times $\tau_e \ll t \ll \tau_d$ where τ_d is the reptation time and τ_e is the entanglement time. At these intermediate times the chain has been smeared out over the tube of diameter d_T (in units of lattice spacings) following an initial Rouse-like decay. The predicted scattering function is

$$S(q,t)/S(q,0) = 1 - \frac{q^2 d_T^2}{36} + q^2 d_T^2 f(\sqrt{q^4\sigma^4 Wt}) \quad (34)$$

with

$$f(u) = \exp(u^2/36)(1 - \mathrm{erf}(u/6)) \quad (35)$$

with erf being the error function. De Gennes derived this formula under the assumption

$$qd_T < 1 \quad (36)$$

Unfortunately, the tube diameter will come out to be about as large as the radius of gyration of the chains and thus the conditions

$$2\pi/R_E < q < 1/d_T \quad (37)$$

where R_E, the end-to-end vector of the chains, leaves only a very small q range if any. We therefore only used our smallest q value $q = 0.15$ to fit the De Gennes prediction, but the outcome is compatible to what comes out of the following description. Ronca[8] augmented the Rouse dynamics by a memory kernel which he determined self-consistently. In his theory he could calculate the dynamic scattering function for all values of qd_T which makes it more versatile for the analysis of experimental or simulational data. His result for the dynamic scattering function is

$$S(q,t)/S(q,0) = \frac{q^2 d_T^2}{24}\int_0^\infty \exp\left(-\frac{q^2 d_T^2}{48} g\left(w, 4\pi Wt \frac{\sigma^4}{d_T^4}\right)\right) dw \quad (38)$$

where the function g is defined as

$$g(w,u) = 2w - \exp(w)\,\mathrm{erfc}\left(\frac{w}{2\sqrt{u}} + \sqrt{u}\right) + \exp(-w)\,\mathrm{erfc}\left(\frac{w}{2\sqrt{u}} - \sqrt{u}\right) \quad (39)$$

erfc being the complementary error function. We used the Ronca prediction for the dynamic scattering function as a fitting function with d_T as free parameter. The rate constant W was taken from the Rouse chains as W^{g_1}. Due to the scattering in the data the resulting d_T values have a huge error bar. The fit works for all the q values, with results differing within the error margins. Figures 10 and 11 show the data for the dynamic structure factor at $1/T = 0$ and $1/T = 1$ in the time range [0, 500 000] Monte Carlo steps (MCS) and the resulting Ronca fit with the mean d_T value at the respective temperature. The resulting fitting curves are reasonably good considering the scatter of the data and the range of length scales fitted. Figure 12 is a plot of the results for the tube diameter as a function of inverse temperature. In spite of the really large error bars one can determine a definite trend for a decreasing tube diameter below a temperature of about $1/T = 0.5$. This is in nice agreement with the findings of the neutron spin echo experiments where the tube diameter started to decrease when the radius of gyration of the chains started to go up due to the increasing chain stiffness. The effect we see in the tube diameter is however much smaller than the one seen in the experiment, whereas the change in the radius of gyration is comparable. This may be attributable to a noticeable density reduction in the experimental system which is absent in the lattice simulation. On the whole, the results however nicely agree, showing that our very simplified model is able to describe the influence of the chain stiffness on the dynamic properties of an entangled polymer melt.

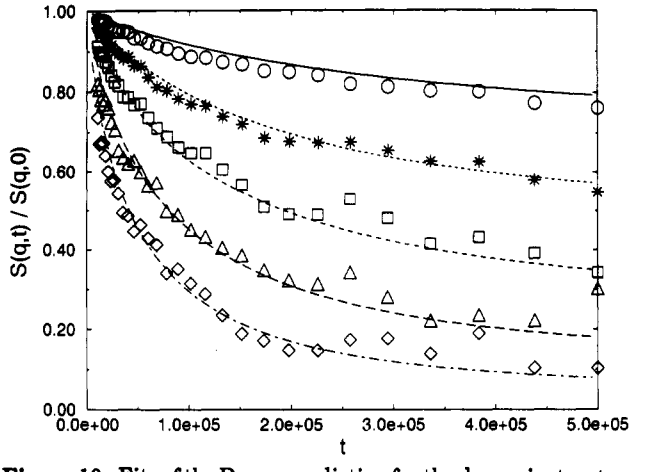

Figure 10. Fits of the Ronca prediction for the dynamic structure factor to the measured data at $1/T = 0$: $q = 0.15$ (circles); $q = 0.2$ (stars); $q = 0.25$ (squares); $q = 0.3$ (triangles); $q = 0.35$ (diamonds).

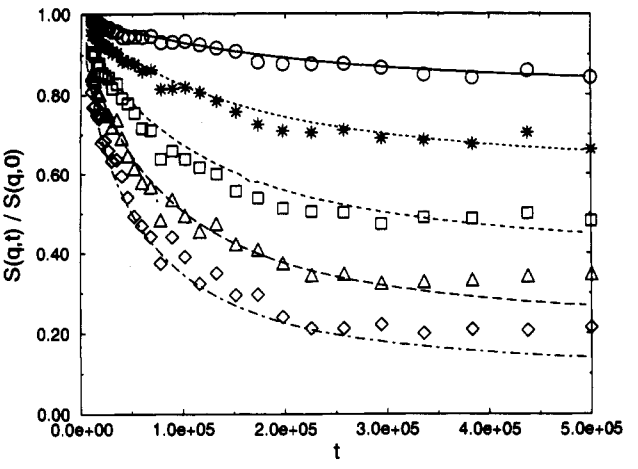

Figure 11. Fits of the Ronca prediction for the dynamic structure factor to the measured data at $1/T = 1$: $q = 0.15$ (circles); $q = 0.2$ (stars); $q = 0.25$ (squares); $q = 0.3$ (triangles); $q = 0.35$ (diamonds).

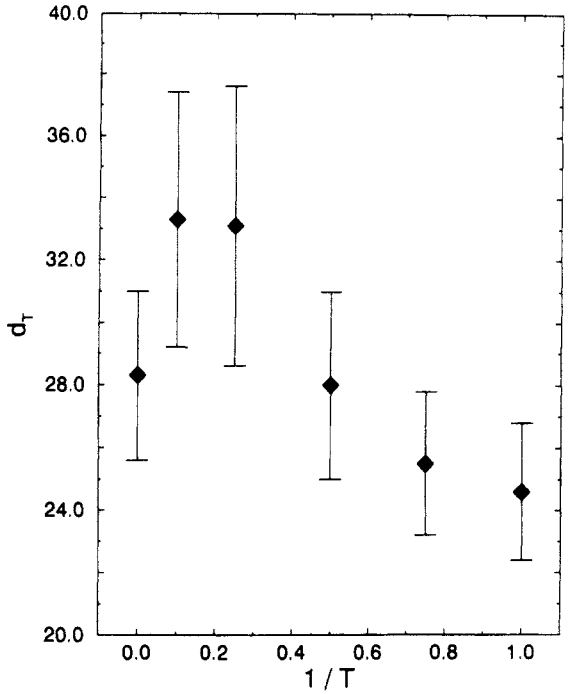

Figure 12. Temperature dependence of the tube diameter obtained from fitting the dynamic structure factor.

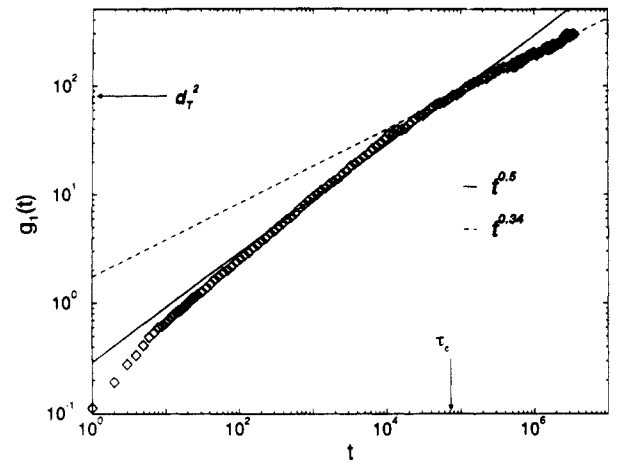

Figure 13. Mean square displacement of the inner monomers, $g_1(t)$, for a chain of length $N = 200$. It displays a crossover from a $t^{0.5}$ to a $t^{0.34}$ behavior at the entanglement time τ_e. Also indicated is the approximate value for the square of the tube diameter d_T^2.

As another possibility to determine the tube diameter, one can look at the mean square displacements of the inner monomers of a chain. Reptation theory predicts a crossover from a $t^{1/2}$ to a $t^{1/4}$ behavior at the entanglement time τ_e. The value of the mean square displacement of the monomers at that time is of the order of the tube diameter. There is a prefactor of the order of unity for which the precise value depends on a more detailed model of the viscoelastic behavior. In ref 15 this crossover for the chains of length $N = 200$ was used to determine an entanglement time $\tau_e \approx 110\,000$ MCS and one could read of a tube diameter $d_T^2 \approx 100$. Figure 13 shows the mean square displacement of inner monomers of a chain of length $N = 200$ for the temperature $T = 1$. Here we measure an entanglement time of $\tau_e \approx 70\,000$ MCS and a tube diameter $d_T^2 \approx 80$. While the absolute value of d_T differs from that determined from the structure factor by a factor of about 2.5, the trend is nevertheless reproduced. Following ref 33, one can discuss invariants involving the tube diameter as they occur in several concurring attempts to describe the reptation dynamics. The general finding $d_T \propto 1/c_N^x$ ($x > 0$) rules out the topological models[31] where $d_T \propto c_N$. The overall picture of the chain motion and structural relaxation certainly nicely confirms the tube model. The invariant occurring in the treatment by Doi and Edwards[5] $d_T^2 G_N^0 / T c_N$ (note that the density ρ is a constant in our simulation) was not accessible to us due to a lack of information about the plateau modulus of our systems. Packing models[10] predict an invariant $d_T c_N$, and scaling models[32] give an invariant $d_T c_N^{a-2}$ with $a \approx 2.3$ (invariants given for constant ρ). Both are in qualitative agreement with our findings, and when one substitutes the values for d_T and c_N, then $d_T c_N$ is constant to within 11% with a slight tendency to increase with decreasing temperature whereas $d_T c_N^{a-2}$ is constant to within 8%. These results differ from the results of the neutron spin echo experiment where the findings on the packing and scaling model were just the other way round. This may be attributable to the different density dependence of these two invariants and a noticeable density variation in the experimental sample in contrast to the situation in the simulation.

Conclusions

We have presented in this paper a Monte Carlo simulation of the bond fluctuation model where bond angle potential produced an increasing chain stiffness with decreasing temperature. For this model we looked at the melt dynamics of short Gaussian chains and showed that the conformational changes of these chains are well described by the Rouse model whereas the overall diffusion of the chains shows a clear signature of a net force acting on the center of mass of the chains. This force is generated by the interaction of the test chains with the surrounding ones and slows down the chain motion at short times. The validity of the Rouse picture shows nicely in the special scaling predicted in the Rouse model of the dynamic structure factor at short times which could be obtained here without free parameters. For the long entangled chains we were able to measure the temperature dependence of the tube diameter by fitting the Ronca prediction to the decay of the dynamic structure factor. The temperature dependence nicely compares to results from a neutron spin echo experiment on poly(ethylene–propylene) and shows that our simple model is able to capture the effect of increasing chain stiffness on the dynamics of entangled polymer melts. An alternative way to measure a length scale approximately equal to the tube diameter out of the mean square displacement of monomers of the chains gave the same qualitative behavior. The dependence of the tube diameter on the chain stiffness clearly rules out topological models where the entanglement distance gets shorter the more a chain can coil.

Acknowledgment. Research was funded by the German Ministry for Research and Technology and Bayer AG under Grant 03M4028. We are indebted to D. Richter and K. Kremer for useful discussions.

References and Notes

(1) Rouse, P. E. *J. Chem. Phys.* **1953**, *21*, 1272.
(2) Ferry, J. D. *Viscoelastic Properties of Polymers*, 3rd ed.; Wiley: New York, 1980.
(3) Richter, D.; Ewen, B.; Farago, B.; Wagner, T. *Phys. Rev. Lett.* **1989**, *62*, 2140.
(4) DeGennes, P. G. *Physics (N.Y.)* **1967**, *3*, 97.
(5) Doi, M.; Edwards, S. F. *The Theory of Polymer Dynamics*; Clarendon Press: Oxford, U.K., 1986.
(6) Doi, M.; Edwards, S. F. *J. Chem. Soc., Faraday Trans. 2* **1978**, *74*, 1789, 1802, 1818.
(7) DeGennes, P. G. *J. Chem. Phys.* **1971**, *55*, 572.
(8) Ronca, G. *J. Chem. Phys.* **1983**, *79*, 1031.

(9) Skolnick, J.; Yaris, R.; Kolinski, A. *J. Chem. Phys.* **1988**, *88*, 1407. Skolnick, J.; Yaris, A. Ibid. **1988**, *88*, 1418. Skolnick, J.; Kolinski, A. *Adv. Chem. Phys.* **1990**, *78*, 223.
(10) Kavassalis, T. A.; Noolandi, J. *Macromolecules* **1988**, *21*, 2869.
(11) Schweizer, K. G. *J. Chem. Phys.* **1989**, *91*, 5802, 5822.
(12) Fixman, M. *J. Chem. Phys.* **1988**, *89*, 3892, 3912.
(13) Kremer, K.; Grest, G. S. *J. Chem. Phys.* **1990**, *92*, 5057.
(14) Paul, W.; Binder, K.; Heermann, D. W.; Kremer, K. *J. Phys. II* **1991**, *1*, 37.
(15) Paul, W.; Binder, K.; Heermann, D. W.; Kremer, K. *J. Chem. Phys.* **1991**, *95*, 7726.
(16) Richter, D.; Baumgärtner, A.; Binder, K.; Ewen, B.; Hayter, B. J. *Phys. Rev. Lett.* **1981**, *47*, 109; **1982**, *48*, 1695.
(17) Higgins, J. S.; Roots, J. E. *J. Chem. Soc., Faraday Trans. 2* **1985**, *81*, 757. Higgins, J. S. *Physica* **1986**, *136B*, 201.
(18) Richter, D.; Farago, B.; Fetters, L. J.; Huang, J. S.; Ewen, B.; Lartigue, C. *Phys. Rev. Lett.* **1990**, *64*, 1389.
(19) Hess, W. *Macromolecules* **1986**, *19*, 1395; **1987**, *20*, 2589; **1988**, *21*, 2620.
(20) Scher, H.; Schlesinger, M. *J. Chem. Phys.* **1986**, *84*, 5922.
(21) Carmesin, I.; Kremer, K. *Macromolecules* **1988**, *21*, 711.
(22) Wittmann, H. P.; Kremer, K. *Comp. Phys. Commun.* **1990**, *61*, 309.
(23) Deutsch, H. P.; Binder, K. *J. Chem. Phys.* **1991**, *94*, 2294.
(24) Lopez-Rodriguez, A.; Wittmann, H. P.; Binder, K. *Macromolecules* **1990**, *23*, 4327.
(25) Wittmer, J. Diplomarbeit, Johannes Gutenberg Universität, Mainz 1991 (unpublished).
(26) Flory, P. J. *Statistical Mechanics of Chain Molecules*; Wiley: New York, 1969.
(27) Wittmann, H. P.; Kremer, K.; Binder, K. *J. Chem. Phys.* **1992**, *96*, 6291.
(28) Paul, W.; Binder, K.; Kremer, K.; Heermann, D. W. *Macromolecules* **1991**, *24*, 6332.
(29) Paul, W. Proceedings of the 1st Tohwa University International Symposium on Slow Dynamics in Condensed Matter, AIP 1992.
(30) Baschnagel, J.; Paul, W.; Binder, K.; Wittmann, H. P. *Proceedings of the 3rd International Workshop on Non-Crystalline Solids*; World Scientific: London, 1992.
(31) Wu, S. *J. Polym. Sci.* **1989**, *27*, 723.
(32) Graessley, W. W.; Edwards, S. F. *Polymer* **1981**, *22*, 1389.
(33) Butera, R.; Fetters, L. J.; Huang, J. S.; Richter, D.; Pyckhout-Hintzen, W.; Zirkel, A.; Farago, B.; Ewen, B. *Phys. Rev. Lett.* **1991**, *66*, 2088. Richter, D.; Farago, B.; Ewen, B.; Fetters, L. J.; Huang, J. S. *Physica B* **1991**, *174*, 209.